Geomechanics and Engineering, *Vol. 13, No. 6 (2017) 1027-1044*
DOI: https://doi.org/10.12989/gae.2017.13.6.1027

Analytical solution and experimental study of membrane penetration in triaxial test

Enyue Ji[1a], Jungao Zhu[*1,2], Shengshui Chen[2b] and Wei Jin[3c]

[1]*Key Laboratory of Ministry of Education for Geomechanics and Embankment Engineering, Hohai University, Nanjing 210098, China*
[2]*Key Laboratory of Failure Mechanism and Safety Control Techniques of Earth-Rock Dam of the Ministry of Water Resources, Nanjing Hydraulic Research Institute, Nanjing 210029, China*
[3]*Chengdu Engineering Corporation Limited, Power China, Chengdu 610072, China*

(Received January 13, 2017, Revised May 3, 2017, Accepted May 18, 2017)

Abstract. Membrane penetration is the most important factor influencing the measurement of volume change for triaxial consolidated-drained shear test for coarse-grained soil. The effective pressure p, average particle size d_{50}, thickness t_m and elastic modulus E_m of membrane, contact area between membrane and soil A_m as well as the initial void ratio e are the major factors influencing membrane penetration. According to the membrane deformation model given by Kramer and Sivaneswaran, an analytical solution of the membrane penetration considering the initial void ratio is deduced using the energy conservation law. The basic equations from theory of plates and shells and the elastic mechanics are employed during the derivation. To verify the presented solution, isotropic consolidation tests of a coarse-grained soil are performed by using the method of embedding different diameter of iron rods in the triaxial samples, and volume changes due to membrane penetration are obtained. The predictions from presented solution and previous analytical solutions are compared with the test results. It is found that the prediction from presented analytical solution agrees well with the test results.

Keywords: membrane penetration; membrane deformation model; isotropic consolidation test; analytical solution

1. Introduction

It is known that the triaxial test is widely used for investigation of stress-strain behavior of soils in laboratory. On the other hand, the triaxial test is often employed to determine the constitutive model parameters used in the designing of earth works by Chen and Wang (2016). It is no doubt that the accuracy of the test results is of great importance for the design of earth-works or the investigation of mechanical behavior of soil. At present, the factors such as end constraint (Omar and Sadrekarimi 2014), sample preparing method and membrane restraint (Raghunandan *et al.*

*Corresponding author, Professor, E-mail: zhujungao@163.com
[a]Ph.D. Student, E-mail: music4388@126.com
[b]Professor, E-mail: sschen@nhri.cn
[c]Engineer, E-mail: 541873892@qq.com

http://www.techno-press.org/?journal=gae&subpage=7 ISSN: 2005-307X (Print), 2092-6219 (Online)

2015) that affect the results of triaxial test are widely studied, besides which, the accuracy of volume changes measured in the test should be taken into consideration. For granular soil, especially coarse-grained soil, the surface of the specimen is uneven, and the thin flexible rubber membrane around the triaxial sample will penetrates the perimeter voids of the sample under confining pressure. This phenomenon is called membrane penetration. In triaxial apparatus, the volume change of soil sample is usually measured by using the volume of drainage from a drainpipe. Apparently, the measured volume change from the drained water of the specimen is not the actual volume deformation of the triaxial sample, as a result, significant errors will appear.

By now, there are extremely few researches studying the membrane penetration. The correction method of membrane penetration is not involved in the specifications for geotechnical test yet, and the problem is far from being solved. Therefore, further research on reliable correction method of membrane penetration is necessary.

From the existing literatures, there are two approaches to the membrane penetration correction, i.e., experimental research and analytical solution.

Newland and Allely (1957) studied membrane penetration behavior using isotropic consolidation tests by the assumption that the triaxial specimen is isotropic. Based on this assumption and triaxial tests of coarse-grained soil, Zhang *et al.* (2003) found that the relationship of confining pressure and penetration volume change can be expressed by hyperbolic function. Roscore *et al.* (1964) proposed a method of embedding copper rods with different diameters into the center of the sand samples to obtain penetration volume changes. Isotropic consolidation drained tests were performed by Frydman *et al.* (1973) by using hollow cylindrical specimens with different thicknesses to study membrane penetration behavior on different particle sizes of glass balls. The relationships between measured volume change and surface area of the sample were used to correct the effect of membrane penetration. Kiekbusch and Schuppener (1977) used the method of coating liquid rubber on the surface of the prepared cylindrical specimen to reduce the influence of membrane penetration. The results show that this method can reduce about 85% penetration effect. By assuming that the cemented specimen had sufficient stiffness to resist deformation under confining pressure, Ali *et al.* (1995) believed that the measured volume changes were equal to the penetration volume changes. Using adhesives, average grain size of 0.31 mm sands was bonded on the surface of cylindrical concrete sample by Raghunandan *et al.* (2013), and the measured volume change equals to penetration volume change based on the assumption that the deformation of the concrete sample can be ignored. Similarly, Haeri *et al.* (2016) used fine sandy coating on gravelly soil specimens to evaluate the effect of membrane penetration of two gravelly specimens.

As mentioned above, the test methods to investigate membrane penetration behavior are mainly for sand. There are few researches on coarse-grained soil, and the test confining pressure is relatively low (less than 200 kPa). The method such as coating liquid rubber or pasting thin copper sheets on the surface will increase the radial rigidity of the sample. In addition, the deformation of copper sheets or liquid rubber will be produced under high confining pressure which will lead to extra penetration. To study membrane penetration behavior through indirect experimental method seems to be more effective, such as the method of embedding copper rod into the center of sample suggested by Roscore *et al.* (1964) mentioned above. Since the use of same height copper rods will increase the end constraint of the sample and thus limits its axial deformation, this method needs to be further improved. Moreover, for coarse-grained soils under high confining pressure, the conclusion of linear relationship between measured volume change and rod diameter obtained by Roscore *et al.* (1964) needs to be further verified by test results.

Yet, as for the existing researches, there are few achievements of analytical solution study. Molenkamp and Luger (1981) proposed three models for membranes with different thicknesses based on elastoplastic theory and the theory of plates and shells. The models provide a good idea for the following research. Baldi and Nova (1984) assumed that the deformation model of the membrane is arc in the plane, and the penetration volume changes under different confining pressures were deduced based on geometric analysis. Kramer and Sivaneswaran (1989) and Kramer *et al.* (1990) deduced the analytical solution of membrane penetration based on an equation of membrane deformation model.

In general, the analytical solutions of membrane penetration above were mostly deduced based on geometric analysis method. In the plane, regular geometry shapes must be assumed, such as parabola and arc, which will result in certain errors compared with the actual membrane deformation. On the other hand, the influence factors involved in the existing analytical solutions need to be further supplemented, and the derivation process needs to be further improved.

In this paper, the mechanism of membrane penetration is analyzed, and the main factors influencing penetration behavior are discussed. Based on the energy conservation law, an analytical solution of membrane penetration is deduced. The penetration volume changes of coarse-grained soil under different confining pressures are obtained from isotropic consolidation tests by the method of embedding iron rods with different diameters into the center of the triaxial samples. Finally, the differences between presented analytical solution and previous analytical solutions are compared with the test results.

2. Mechanism and main factors of membrane penetration

2.1 Mechanism of membrane penetration

The application of confining pressure causes membrane to be penetrated into the pores of soil particles on the sample surface in triaxial test. Fig. 1 shows the schematic diagram of membrane penetration. In the following of this paper the “surface soil” refers to a layer of soil particles which contact with the membrane directly for a specimen, as shown in Fig. 1, besides which is the “internal soil”. It can be seen that the degree of penetration increases with the increase of confining pressure. Owing to the close contacting between surface soil particles, the membrane will only

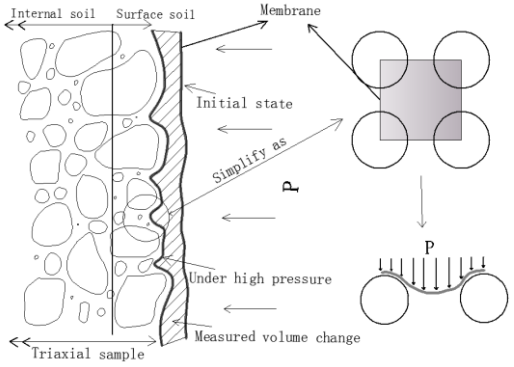

Fig. 1 Schematic diagram of membrane penetration in triaxial test

penetrate into the pores of surface soil. This phenomenon determines that the properties of the internal soil, such as particle size or particle content will not affect the final penetration volume change. The derivation of analytical solution in this paper below is also based on the assumption that the membrane only penetrates into the pores of surface soil. As shown in Fig. 1, any four soil particles which are in direct contact with the membrane can be simplified as a unit sphere group, and will be further analyzed in the following of this paper.

For drained triaxial test of saturated soil sample, the measured volume change of triaxial sample should consist of volume deformation of soil and membrane penetration volume change, which can be written by

$$\Delta V = \Delta V_s + \Delta V_m \tag{1}$$

where DV is the measured volume change of the sample, DV_s is the volume change of soil, and DV_m is the volume change due to membrane penetration. Apparently, DV can be measured directly from the drained water of the specimen, but DV_s and DV_m can't be obtained through the test immediately. If is taken as the ignoring of membrane penetration may result in over measurement during the test.

2.2 Main factors of membrane penetration

A number of researchers (Bohac and Feda 1992, Lade 2016) believed that the effective pressure p is the most important factor influencing membrane penetration, and the degree of membrane penetration is much greater under high pressure than that at initial state, as shown in Fig. 1.

Besides the effective pressure, particle size is also one of the major factors. Frydman *et al.* (1973) pointed out that the impact of particle size is the main factor influencing penetration through hollow cylindrical tests. The bigger the particle size is, the greater the influence will be. When the average particle size is less than 0.1-0.2 mm, the influence is small enough to be ignored. He also held the point that the factors like relative density, particle shape and particle property bring little influence. Sun *et al.* (2006) used digital image measurement system to study membrane penetration. According to the test results, it can be concluded that the penetration volume changes of IOS standard sand increase with the increasing average particle size d_{50}. In particular, the test results from Noor *et al.* (2012) indicated that the penetration volume change increases about two times as the average particle size increases from 0.3 mm to 2.0 mm.

Another major factor is the property of the rubber membrane which mainly refers to membrane's thickness and elastic modulus. Kiekbusch and Schuppener (1977) performed a lot of tests to study the impact of membrane thickness on membrane penetration. The test results show that when the thickness increases by 5 times, the penetration volume change will reduce by about 50% under the same confining pressure. Moreover, the contact area A_m between membrane and the surface of specimen is also a factor influencing the final penetration. Usually, the penetration volume change is proportional to A_m.

Besides the above-mentioned factors, the authors believe that the density of soil should also be an important factor, which refers to the initial density of the sample. As shown in Fig. 2, the distance between two certain particles on the sample surface under the loose state is larger than that under the dense state. For the same effective pressure, membrane will penetrate the voids of the sample easier under loose state than that under dense state. Comparatively, the penetration volume change will be larger for specimen under loose state.

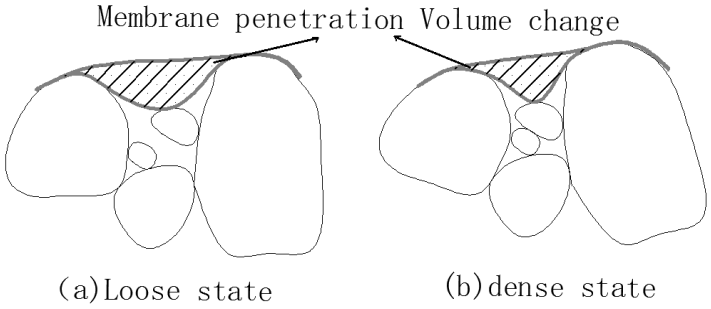

Fig. 2 Soil particle distribution under different states

To introduce the initial density into quantitative derivation possibly, the initial density can be expressed by the initial void ratio *e*. Bopp and Lade (2005) held the similar view that the initial void ratio has considerable effect on membrane penetration. For the analytical solution deduction, *e* should be taken into account.

According to the analyses above, it is concluded that the main factors affecting membrane penetration are effective pressure *p*, average particle size d_{50}, thickness tm and elastic modulus E_m of membrane, contact area A_m, initial void ratio *e*. The factors such as particle shape, particle property, particle arrangement are assumed not to be taken into account in this paper.

3. Analytical solution of membrane penetration

3.1 Analysis of membrane deformation model

The deformation model of the membrane determines the final penetration volume change. First and foremost, to identify a reasonable deformation model before deriving the analytical solution is necessary. As mentioned above in Fig. 1, the particle size of the soil is supposed equal to the average particle size d_{50} in the unit sphere group, and the effective pressure *p* distributes uniformly on the surface of the unit membrane. It is also assumed that the uniform array of four spheres is in a horizontal plane and the central axes of the spheres are parallel to each other.

The deformation models suggested by Molenkamp and Luger (1981), Baldi and Nova (1984) as well as Kramer *et al.* (1990) are shown in Fig. 3. The four corners of the unit membrane cell are coinciding with the apexes of the four spheres in Fig. 3.

Molenkamp and Luger (1981) assumed that the deformation model of the unit membrane is in accordance with the schematic diagram of Fig. 3 (a). The deformation equation can be expressed by a parabolic equation in plane. Apparently, the unit membrane will exceed the boundary of the spheres as the effective pressure reaches a certain value, resulting in overlapping. The deformed shape of the unit membrane also violates the displacement boundary conditions. Baldi and Nova (1984) held the view that the deformation model is similar to a cylindrical surface. The deformation curve can be described by an arc in plane. Similarly, this deformation model does not conform to the actual deformed shape and also does not obey the displacement boundary conditions.

To make the corners of the membrane on the unit sphere group deform along the sphere boundaries as much as possible, and to make the membrane deformation model be as close as

possible to the actual deformed shape, the membrane deformation model proposed by Kramer *et al.* (1990) is shown in Fig. 3(c). The model is obtained by a superposition of orthogonal cosine wave functions with wavelength a in x-y-z plane. It can be seen that the deformed shape is closer to the actual deformed shape, but it does not mean it is precise.

In Fig. 4, a space coordinate axis x-y-z locates in the unit sphere group with x and y axes passing through the center line of spheres is established. The center distance between the neighboring spheres is a, the sphere diameter is d_{50}, and the thickness and the elastic modulus of the membrane are t_m and E_m, respectively.

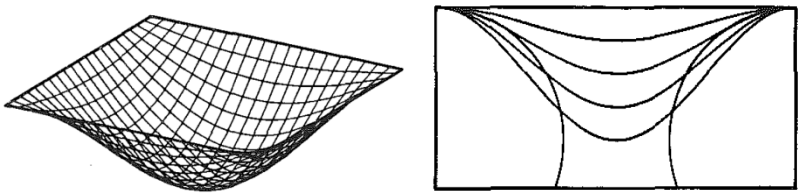

(a) Molenkamp and Luger (1981)

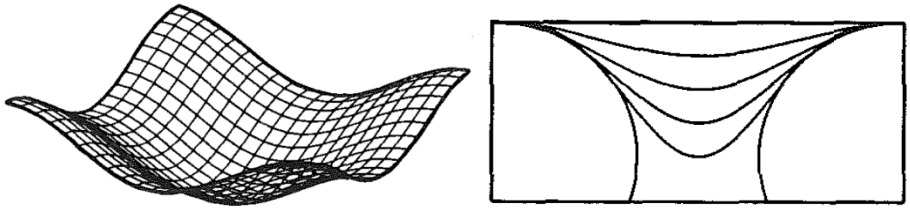

(b) Baldi and Nova (1984)

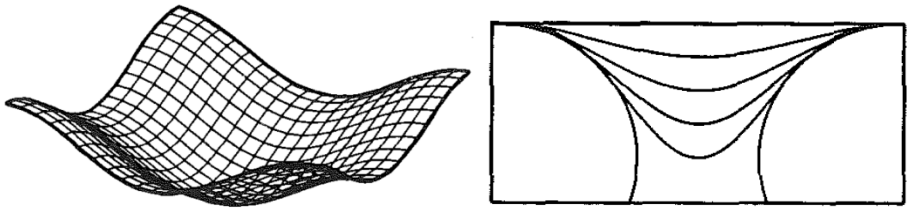

(c) Kramer *et al.* (1990)

Fig. 3 Schematic diagram of membrane deformations

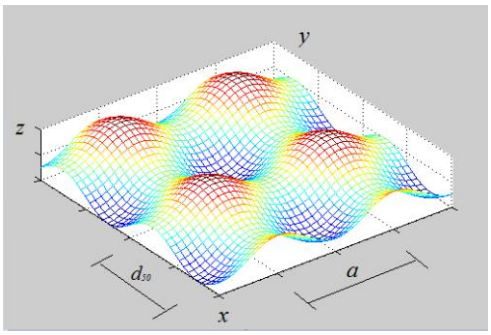

Fig. 4 Unit sphere group under a space coordinate system

The deformation equation suggested by Kramer *et al.* (1990) is given by

$$\omega(x,y)=\omega_0(1-\frac{1}{2}\cos\frac{2\pi x}{a}-\frac{1}{2}\cos\frac{2\pi y}{a})-\alpha\omega_0(1-\frac{1}{2}\cos\frac{4\pi x}{a}-\frac{1}{2}\cos\frac{4\pi y}{a}) \tag{2}$$

where $\omega(x,y)$ is the deflection of the deformed surface in z direction as shown in Fig 4. ω_0 is the mean membrane deflection, α is an empirical coefficient which makes the deformed shape more accurate and is determined empirically to make the membrane does not deflect at the corners. The maximum value of the equation is ω_0 $(2-\alpha)$ at the center of the unit sphere group.

α can be expressed by (Kramer *et al.* 1990)

$$\alpha=0.15\left(\frac{pd_{50}}{E_m t_m}\right)^{0.34} \tag{3}$$

Define the unit volume change due to membrane penetration as

$$\varepsilon_{vm}=\Delta V_m / A_m \tag{4}$$

where A_m is the contact area between membrane and triaxial sample. Divide the membrane into countless differential elements dA_m, the space between all differential elements and deformed surface in Fig. 4 constitutes the volume change due to membrane penetration. Then, the equation is given by

$$\int_A \omega_0 dA_m=\Delta V_m \tag{5}$$

Consequently, the mean deflection ω_0 is equal to the unit penetration volume change, and will be deduced in next section.

3.2 Analytical solution to membrane penetration based on the energy conservation law

The solution to large deflection of a plate under uniform pressure was given by Reddy (2006) based on the theory of plates and shells. Ignoring its bending stiffness, the plate can be simplified to a unit membrane with thickness t_m, elastic modulus E_m and Poisson's ratio v. The internal force and the strain of a certain element from the unit membrane is N_x, N_y, N_{xy} and ε_x, ε_x, γ_{xy} in x-y plane, respectively.

The physical equations from the elastic mechanics are given by

$$\begin{aligned}\varepsilon_x&=(N_x-vN_y)/E_m t_m\\ \varepsilon_y&=(N_y-vN_x)/E_m t_m\\ \gamma_{xy}&=N_{xy}/G_m t_m\end{aligned} \tag{6}$$

where G_m is the shear modulus of the membrane which is expressed as

$$G_m=\frac{1}{2}E_m/(1+v) \tag{7}$$

The compatibility equations from the theory of plates and shells are given by

$$\varepsilon_x = \frac{\partial u}{\partial x} + \frac{1}{2}\left(\frac{\partial \omega}{\partial x}\right)^2$$
$$\varepsilon_y = \frac{\partial v}{\partial y} + \frac{1}{2}\left(\frac{\partial \omega}{\partial y}\right)^2 \tag{8}$$
$$\gamma_{xy} = \frac{\partial u}{\partial y} + \frac{\partial v}{\partial x} + \frac{\partial \omega}{\partial x}\frac{\partial \omega}{\partial y}$$

where *u*, *v*, *w* are displacements of *x*, *y*, *z* directions, respectively. It should be noted that Molenkamp *et al.* (1990) ignored the incremental displacement of *x* and *y* directions in order to simplify the calculation, that is, the first equations from the right side of Eq. (8) are neglected.

The strain energy *V* of the membrane is

$$V = \frac{1}{2}\iint \left(N_x \varepsilon_x + N_y \varepsilon_y + N_{xy}\gamma_{xy}\right) d_x d_y \tag{9}$$

Substituting Eq. (6) into Eq. (9), *V* can be obtained as

$$V = \frac{E_m t_m}{2(1-\nu^2)} \iint \left[{\varepsilon_x}^2 + {\varepsilon_y}^2 + 2\nu\varepsilon_x\varepsilon_y + \frac{1}{2}(1-\nu){\gamma_{xy}}^2 \right] d_x d_y \tag{10}$$

where *v* can be taken as 0.5 generally (Timoshenko and Goodier 1970). For the displacements of *u* and *v*, the equations can be obtained by the sine cosine wave functions (Reddy 2006) which are expressed as

$$u = c \sin\frac{\pi x}{a}\cos\frac{\pi y}{2a} \tag{11}$$

$$v = c \sin\frac{\pi y}{a}\cos\frac{\pi x}{2a} \tag{12}$$

where *c* is the horizontal amplitude. The value change of *c* only produces the change of the horizontal displacement and the vertical load does not produce work. Thus, an equation is given by

$$\frac{\partial V}{\partial c} = 0 \tag{13}$$

Substituting Eqs. (2), (6), (7) and (10) into Eq. (13), then *c* is obtained by

$$c = 0.21{\omega_0}^2\left(\frac{1}{3a} + \frac{64\alpha}{15a}\right) \tag{14}$$

The work done by vertical pressure *p* on membrane should be equal to the membrane strain energy based on the principle of virtual work, then it gives

$$\frac{\partial V}{\partial \omega_0}\delta\omega_0 = \int_{-a}^{+a}\int_{-a}^{+a} p\delta\omega_0 \left[(1 - \frac{1}{2}\cos\frac{2\pi x}{a} - \frac{1}{2}\cos\frac{2\pi y}{a}) - \alpha(1 - \frac{1}{2}\cos\frac{4\pi x}{a} - \frac{1}{2}\cos\frac{4\pi y}{a}) \right] d_x d_y \tag{15}$$

In Eq. (15), the left formula is the strain energy of the membrane, and the right formula is the work done by p. Combining the Eqs. (10), (14) and (15), ω_0 can be obtained as

$$\omega_0 = \varepsilon_{vm} = a\left(\frac{1-\alpha}{4M}\right)^{1/3}\left(\frac{pa}{E_m t_m}\right)^{1/3} \tag{16}$$

where m=324.7α^4+237.3α^2−3.5α+20.2, α is shown in Eq. (3).

The void ratio e can be expressed as

$$e = (V_t - V_s)/V_s \tag{17}$$

where V_t is the volume of the sample, V_s is the total volume of soil particles.

Assuming a cubic cell in the triaxial sample with N_3 particles uniformly arranged in it, and the center distance of the adjacent particles is a, thus e can be expressed as

$$e = \frac{N^3\lambda^3 d^3 - N^3 V_s}{N^3 V_s} = \frac{8}{\pi}\lambda^3 - 1 \tag{18}$$

Then λ can be obtained

$$\lambda = 0.732(1+e)^{\frac{1}{3}} \tag{19}$$

a can be given by

$$a = \lambda d_{50} = 0.732d(1+e)^{\frac{1}{3}} \tag{20}$$

Substituting Eq. (20) into Eq. (16), ε_{vm} can be derived as

$$\varepsilon_{vm} = 0.66d_{50}(1+e)^{\frac{4}{9}}\left(\frac{1-\alpha}{4M}\right)^{1/3}\left(\frac{pd_{50}}{E_m t_m}\right)^{1/3} \tag{21}$$

In Eq. (21), ε_{vm} is the unit volume change due to membrane penetration to be derived in this paper. For a sample of triaxial CD test, the penetration volume change can be expressed as

$$V_m = 0.66\frac{4d_{50}}{D}(1+e)^{\frac{4}{9}}\left(\frac{1-\alpha}{4M}\right)^{1/3}\left(\frac{pd_{50}}{E_m t_m}\right)^{1/3} \tag{22}$$

where D is the diameter of the triaxial sample.

4. Membrane penetration tests

4.1 Test principle

To investigate the penetration behavior and verify the presented solution, penetration test is performed on a coarse-grained soil in this study. As shown in Fig. 5, the height of the triaxial test

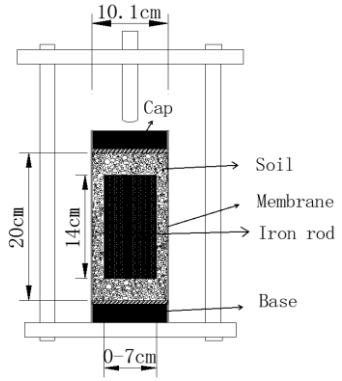

Fig. 5 Schematic diagram of triaxial Isotropic consolidation test

sample is 20 cm, and the diameter of which is 10.1 cm. Penetration volume changes are obtained from isotropic consolidation tests by the method of embedding iron rods of different diameters in the center of triaxial samples.

In Fig. 5, the sample refers to a cylinder which contains soil and an iron bar. The volume of the soil and the volume of the iron rod consists the total volume of the sample. Apparently, when the diameter of the iron bar changes to 0, the sample is filled with soil entirely.

According to Eq. (1), if volume of soil is equal to 0, the measured volume change should equal the penetration volume change theoretically. Nevertheless, the soil volume cannot possibly be equal to 0 in the actual triaxial test, and the penetration volume change cannot be measured directly. If DV_m can remain be unchanged for the samples with different diameters of iron rods under the same confining pressure, the relationship between DV_s and DV can be established since the iron rods with different diameter lead to the change of DV_s. Moreover, the measured volume changes of the sample in the situation that the soil volume is 0 can further be obtained.

In Fig. 2, membrane will only penetrate into the pores of the surface soil. The particle content of internal soil will not affect DV_m based on the assumption that the specification of the rubber membrane, particle size, the grain arrangement and effective pressure should be the same. In other words, according to this assumption, it can be considered that DV_m of samples with different diameter iron rods can keep constant under the same confining pressure. As a result, the above-mentioned relationship between DV_s and DV can be established.

Based on the test principle and hypothesis above, DV_s is changed by embedding iron rods with different diameters in the center of triaxial specimens. Through isotropic consolidation tests, DV of triaxial samples with different diameter iron rods under different confining pressures are measured. The relationships between DV_s and DV are established to deduce DV_m under each confining pressure when the volume of soil is equal to 0.

4.2 Test programs

Four kinds of programs (samples with iron bars of different diameters) are operated by isotropic consolidation tests. The diameter of iron rod in the center of the sample is 0 (no iron bar in the sample), 2.5, 4.5, 7 cm, respectively, and the length of iron bars are all 14 cm as is shown in Fig. 6. In addition, three parallel tests were carried out for each program. There are 12 samples altogether.

(a) 2.5 cm iron bar (b) 4.5 cm iron bar (c) 7 cm iron bar

Fig. 6 Triaxial samples with iron bars of different diameters

As mentioned above, Roscore *et al.* (1964) investigated membrane penetration behavior by embedding copper rods with different diameters in the center of the sand sample. The disadvantage is that the copper rod which has the same height with the triaxial sample will limit the development of the axial deformation of the sample inevitably. Moreover, the use of rigid top cap will concentrate the stress on the copper rod, and the vertical stress of the soil around the copper rod will be lower than the corresponding radial stress. Consequently, the sample will no longer be in an isotropic consolidation state which is unreasonable. In this study, the embedded iron rods are shorter than the sample, that is, 3 cm height is reserved for the top and bottom of the sample respectively. The sample has 6 cm compression height which will reduce the limit of axial deformation.

After the saturation, the volume change and axial deformation can be measured as the confining pressure applied to 100 kPa. The confining pressure is gradually increased to 2MPa and the increment of each step is 100 kPa. The volume changes and axial deformation of each stage are measured.

4.3 Soil used in the test

The soil used in the test is coarse-grained soil from a rockfill dam, and the parent rock is granite. The maximum diameter of iron rod is 7 cm while the diameter of sample is 10.1 cm. In order to minimize the size effect, the maximum diameter of the particle is 10 mm and the minimum particle size is 0.1 mm in the test. The grading curve is shown in Fig. 7, c_u=5.4, c_c=3.3, d_{30}=2.67 mm, d_{50}=4.42 mm and d_{60}=5.37 mm, respectively.

To make the preparation of samples easier, the relative density of soil selected in the test is relatively low. The basic parameters of the soil used are shown in Table 1. Different specifications of specimen makers with different base plates should be made in order to achieve higher density, which will be researched in further study. Taking account that the coarse-grained soil can puncture

the membrane easily under high confining pressure, the whole thickness of the membranes is 2.2 mm with inner 0.2 mm and outer 2 mm. The total elastic modulus of the two membranes is 1.608 MPa according to uniaxial tensile test (Komurlu *et al.* 2016) without considering the interaction between the inner and the outer membrane.

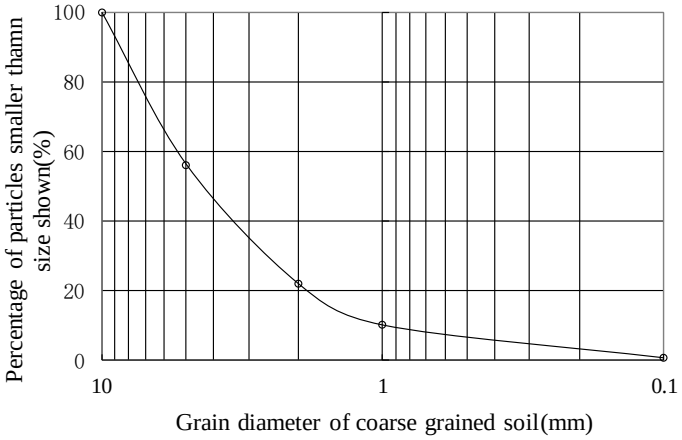

Fig. 7 Grading curve of the coarse-grained soil in the test

Table 1 Parameters of coarse-grained soil in the test

Initial void ratio *e*	Maximum dry density ($g \cdot cm^{-3}$)	Minimum dry density ($g \cdot cm^{-3}$)	Dry density in test ($g \cdot cm^{-3}$)	Relative density (%)
0.53	2.03	1.56	1.76	50%

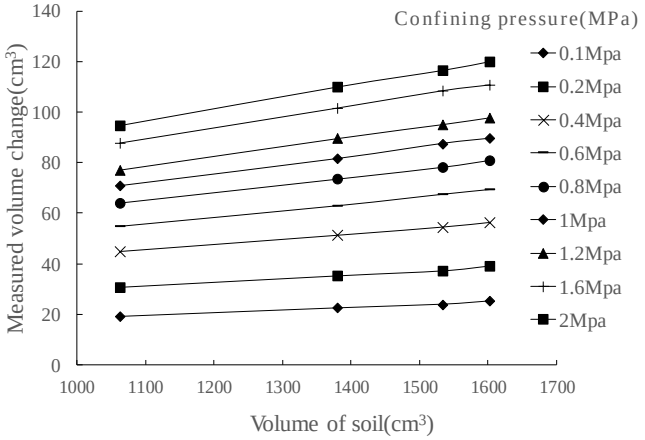

Fig. 8 Relation curves of measured volume change versus volume of soil

Table 2 Membrane penetration under each confining pressure

Confining pressure (MPa)	Measured volume change (cm^3)	Penetration volume change(cm^3)	Proportion of penetration (%)
0.1	25.2	7.8	31.0

Table 2 Continued

Confining pressure (MPa)	Measured volume change (cm^3)	Penetration volume change (cm^3)	Proportion of penetration (%)
0.2	39.2	15.0	38.3
0.4	56.3	22.9	40.7
0.6	69.5	27.6	39.7
0.8	80.9	31.3	38.7
1	89.5	34.4	38.4
1.2	97.6	37.0	37.9
1.6	110.6	41.8	37.8
2	120.1	45.0	37.5

4.3 Test results

Fig. 8 shows the relationships of measured volume changes against volumes of the soil with the confining pressure changing from 0.1 MPa to 2 MPa. It should be noted that, to minimize the randomness of soil particle arrangement to reduce the error of the same program, three parallel tests were done of each program in Fig.8. Consequently, the measured volume change is a corresponding average value of three parallel tests. In addition, since the incremental confining pressure is 100 kPa, and it is difficult to distinguish 20 curves, only 9 curves of the confining pressure in the range from 0.1 MPa to 2 MPa are given in Fig. 8.

It can be seen that the linear relationships between measured volume changes and soil volumes are very obvious from Fig. 8, and the minimum correlation coefficient R_2 of the fitting curves is 0.989. Linear fitting the test points under each confining pressure, the measured volume changes can be obtained when the soil volumes are equal to 0 (the intersection of the curves and the Y axis), which are the membrane penetration volume changes under each confining pressure.

Table 2 shows values of measured volume changes and penetration volume changes as well as the proportions of penetration in real-time measured volume change. With the increase of confining pressure, the penetration volume changes increase gradually. Further, the penetration volume changes increase rapidly at the beginning of the test, the increment of which become slowing down after about 0.8MPa.

From the whole test, the proportion of penetration volume change in real-time measured volume change can reach 31.0%-40.7%. Zhang *et al.* (2003) also mentioned that the penetration accounts for about 30%-50% of the whole measured volume change. Apparently, there exists significant error if the measured volume change is not corrected in the conventional triaxial test.

5. Verification of analytical solutions

To compare the difference between the presented analytical solution and the previous analytical solutions with test results, several analytical solutions from previous studies are listed. A solution by Molenkamp and Luger (1981) employs

$$\varepsilon_{vm} = 0.16 d_{50} \left(\frac{p d_{50}}{E_m t_m} \right)^{\frac{1}{3}} \tag{23}$$

Baldi and Nova (1984) suggested a solution written as

$$\varepsilon_{vm} = 0.125 d_{50} \left(\frac{p d_{50}}{E_m t_m} \right)^{\frac{1}{3}} \tag{24}$$

Kramer and Sivaneswaran (1989) gave a solution by

$$\varepsilon_{vm} = 0.231 d_{50} \left(\frac{p d_{50}}{E_m t_m} \right)^{\frac{1}{3}} \tag{25}$$

An improved solution by Kramer *et al.* (1990) is expressed as

$$\varepsilon_{vm} = 0.395 d_{50} \left(\frac{1-\alpha}{5+64\alpha^2+80\alpha^4} \right)^{\frac{1}{3}} \left(\frac{p d_{50}}{E_m t_m} \right)^{\frac{1}{3}} \tag{26}$$

where α is shown in Eq. (3).

Fig. 9 shows the relationships between penetration volume changes and confining pressures of the presented analytical solution and the previous analytical solutions. The overall trend of the five analytical solutions is the same, that is, the penetration volume changes increase with the increasing confining pressures. There are, however, significant differences between the solutions of Eqs. (24), (25), (26) and the test data, while the difference between Eq. (21) presented in this study as well as Eq. (23) and the test result is relatively small. The relation curves of Eqs. (21) and (23) are mostly overlapped with test results under the confining pressure less than 0.7 MPa of confining pressure. When the confining pressure is more than 0.7MPa, the predictions of Eqs. (21) and (23) deviate from the test data. Furthermore, as the confining pressure reaches 2MPa, the

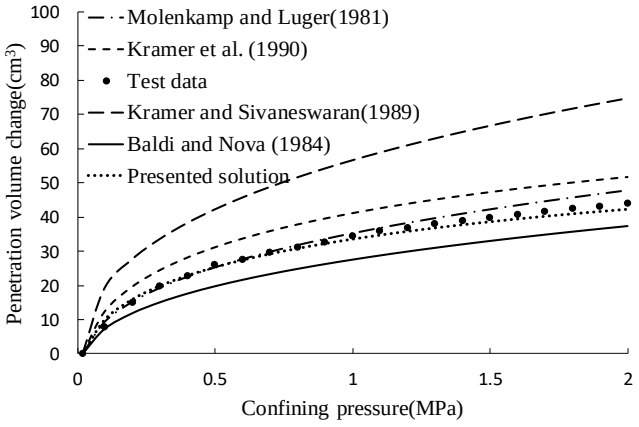

Fig. 9 Relation curves of analytical solutions versus test data

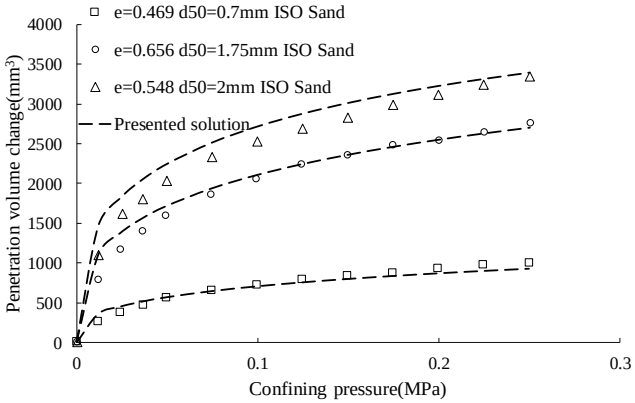

Fig. 10 Relation curves of analytical solutions versus test data from Sun *et al.* (2006)

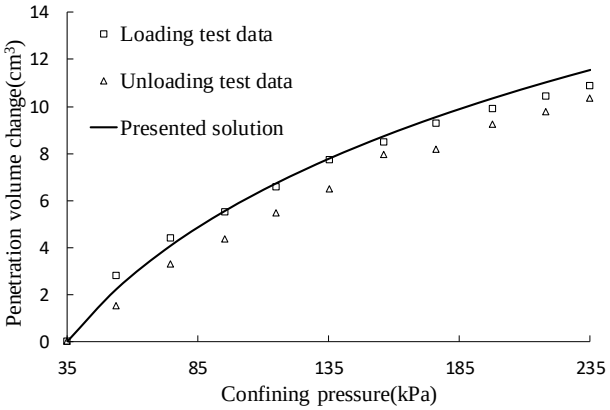

Fig. 11 Relation curves of analytical solutions versus test data from Ali *et al.* (1995)

difference between the value of Eq. (21) presented in this study and the test data is merely 1.7 cm^3 which accounting for 3.8% of the total measured volume change. By contrast, the difference between the value of Eq. (23) from Molenkamp and Luger (1981) and the test data is 3.7 cm^3, accounting for 8.2% of the total measured volume change. In general, the presented analytical solution satisfies the test results better than the above solutions and is proved to be reasonable. The possible reason that the calculation values of Eq. (21) is a bit lower than the test data is that the empirical coefficient α in Eq. (21) is overestimated under high confining pressure. In order to improve the accuracy of Eq. (21), the authors think that more tests should be done to correct α.

Sun *et al.* (2006) applied membrane penetration tests on sands with different particle size and gradation based on the digital image measurement system. The relationships between penetration volume changes and the confining pressures were analyzed. The analytical solution Eq. (24), which is given by Baldi and Nova (12), was pointed out to be obviously different from the test result, and Eq. (24) is corrected according to the test results by Sun *et al.* (2006). In the test, E_m is 1.3 MPa and t_m is 0.25 mm. The sample size is ϕ 39.1 mm×80 mm. The relation curves between presented analytical solution and the test data of Sun *et al.* (2006) are shown in Fig. 10. For ISO standard sands with d_{50} of 0.7 mm and 1.75 mm, the results of presented analytical solution satisfy the test results very well. While, for ISO standard sand with d_{50} of 2 mm, some differences

between the calculated values and the test data exist which can be up to 254 mm^3, accounting for 7.6% of the total measured volume change. In general, the actual membrane penetration can be calculated accurately by the presented analytical solution on the standard sand with different initial void ratios and grain sizes compared to other analytical solutions as mentioned above. The results from Eqs. (23)-(26) cannot reflect the volume changes due to penetration caused by initial void ratio. The differences between calculated values of previous solutions and test data are also very large which are not showed in Fig. 10.

Ali *et al.* (1995) used cemented samples to apply membrane penetration test. The cemented sample is suggested to be sufficiently rigid due to the cementation that the deformation of the sample is assumed to be 0. Thus, the measured volume change is entirely due to membrane penetration. In the tests, the confining pressure was increased from 35 to 235 kPa and then decreased to 35 kPa. E_m is 1.195MPa and t_m is 0.42 mm suggested in the test, the diameter and height of sample is 10 cm and 20 cm, respectively. Fig. 11 shows a comparison curve of the penetration volume change from the presented solution with test results for increasing confining pressure from 35 to 235 kPa. For the loading test data, the presented solution agrees well while relatively big errors exist in the prediction of penetration in unloading test. During unloading test, unrecoverable deformation of the membrane occurs for the reason that the membrane is elastic-plastic material. For simplification, the presented solution is deduced assumed that the membrane is elastic material. As a consequent, errors exist in the prediction in unloading test.

It should be pointed out that the analytical solution derived in this study is based on the assumption that the soil particle sizes are equal to the average particle diameter d_{50}, which may only apply to the soil with good gradation. For the soil with poor gradation, the non-uniform coefficient c_u and the curvature coefficient c_c may be used to improve the analytical solution.

In addition, for coarse-grained soil, the influence of particle breakage under high confining pressure need to be taken into consideration in the subsequent research. However, the sieving analysis tests are not applied in this study after completion of the isotropic consolidation tests. The relationships between breaking rates and confining pressures cannot be definitely established to modify the presented solution which need more researches. Furthermore, as mentioned above, the relative density used in this study is only 50%. It is difficult to prepare the sample with higher density owing to the iron bars with different diameters, therefore, the different specifications of the sample reparation device are needed in further study.

Generally, from the existing test results, the presented analytical solution is verified to be effective for membrane penetration correction and need to be further validated by more membrane penetration tests in the following study.

6. Conclusions

In this paper, the analytical solution of membrane penetration considering the initial void ratio is deduced based on the theory of plates and shells as well as the elastic mechanics. By embedding iron rods with different diameters in triaxial specimens, the penetration volume changes under different confining pressures are obtained. Finally, the differences between presented analytical solution and previous analytical solutions are compared with the test results. The preliminary conclusions and suggestions are as follows:

• The main factors affecting membrane penetration are effective pressure p, the average particle size d_{50}, thickness t_m and elastic modulus E_m of membrane, contact area A_m, as well as the initial

void ratio *e*.

• Based on the membrane deformation model given by Kramer and Sivaneswaran, the analytical solution of the membrane penetration is deduced from the law of energy conservation based on the theory of plates and shells as well as the basic equations of elastic mechanics. In the deviation the initial void ratio of specimen is taken into account.

• It is proved that the penetration volume changes of coarse-grained soils under different confining pressures can be obtained by embedding iron rods with different diameters in the triaxial specimens. The proportion of penetration volume change in real-time measured volume change can reach about 31.0%-40.7%.

• In general, the calculated results of the presented analytical solution are in better agreement with the test data than that of other previous solutions, which is proved to be reasonable.

Acknowledgments

The authors gratefully acknowledge the financial support from a research grant (No. 51479052) from NSFC, research grant (No. B13024) from the 111 Project and a research grant (No. YK915001) from the Open Foundation of Key Laboratory of Failure Mechanism and Safety Control Techniques of Earth-rockfill Dam of the Ministry of Water Resources.

References

Ali, S.R., Pyrah, I.C. and Anderson, W.F. (1995), "A novel technique for evaluation of membrane penetration", *Geotech*., **45**(3), 545-548.

Baldi, G. and Nova, R. (1984), "Membrane penetration effects in triaxial testing", *J. Geotech. Eng*., **110**(3), 403-420.

Bohac, J. and Feda, J. (1992), "Membrane penetration in triaxial tests", *Geotech. Test. J*., **15**(3), 288-294.

Bopp, P.A. and Lade, P.V. (2005), "Relative density effects on undrained sand behavior at high pressures". *Soils Found.*, **45**(1), 15-26

Cheng, X.L. and Wang, J.H. (2016), "An elastoplastic bounding surface model for the cyclic undrained behaviour of saturated soft clays", *Geomech. Eng*., **11**(3), 325-343.

Frydman, S., Zeitlen, J.G. and Alpan, I. (1973), "The membrane effect in triaxial testing of granular soils", *J. Test. Eval*., **1**(1), 37-41.

Haeri, S.M., Raeesi, R. and Shahcheraghi, S.A. (2016), "Elimination of membrane compliance using fine sandy coating on gravelly soil specimens", *Proceedings of the 5th International Conference on Geotechnical Engineering and Soil Mechanics*, Tehran, Iran, November.

Kiekbusch, M. and Schuppener, B. (1977), "Membrane penetration and its effect on pore pressures", *J. Soil Mech. Found. Div*., **103**(11), 1267-1279.

Komurlu, E., Kesimal, A. and Demir, S. (2016), "Experimental and numerical analyses on determination of indirect (splitting) tensile strength of cemented paste backfill materials under different loading apparatus", *Geomech. Eng*., **10**(6), 775-791.

Kramer, S.L. and Sivaneswaran, N. (1989), "A nondestructive, specimen-specific method for measurement of membrane penetration in the triaxial tests", *Geotech. Test. J*., **12**(1), 50-59.

Kramer, S.L., Sivaneswaran, N. and Davis, R.O. (1990), "Analysis of membrane penetration in triaxial test", *J. Eng. Mech*., **116**(4),773-789.

Lade, P.V. (2016), *Triaxial Testing of Soils*, John Wiley & Sons, West Sussex, U.K.

Molenkamp, F. and Luger, H.J. (1981), "Modelling and minimization of membrane penetration effects in

tests on granular soils", *Geotech*., **31**(4), 471-486.
Newland, P.L. and Allely, B.H. (1957), "Volume changes in drained taixial tests on granular materials", *Geotech*., **7**(1), 17-34.
Noor, M.J.M., Nyuin, J.D. and Derahman, A. (2012), "A graphical method for membrane penetration in triaxial tests on granular soils", *J. Inst. Eng*., **73**(1), 23-30.
Omar, T. and Sadrekarimi, A. (2014), "Effects of multiple corrections on triaxial compression testing of sands", *J. GeoEng*., **9**(2), 75-83.
Raghunandan, M.E., Juneja, A. and Hsiung, B. (2013), "Preparation of reconstituted sand samples in the laboratory", *J. Geotech. Eng*., **6**(1), 125-131.
Raghunandan, M.E., Sharma, J.S. and Pradhan, B. (2015), "A review on the effect of rubber membrane in triaxial tests", *Arab. J. Geosci*., **8**(5), 3195-3206.
Reddy, J.N. (2006), *Theory and Analysis of Elastic Plates and Shells*, Taylor and Francis Group, New York, U.S.A.
Roscoe, K.H., Schofield, A.N. and Thurairajah, A. (1964), *An Evaluation of Test Data for Selecting a Yield Criterion for Soils*, ASTM International, West Conshohocken, Pennsylvania, U.S.A.
Sun, Y.Z., Shao, L.T., Wang, Z.P. and Wang, Q.M. (2006). "Study on membrane penetration in sandy soil specimens based on digital image measurement system", *J. Rock Mech. Eng*., **25**(3), 618-622.
Timoshenko, S.P. and Goodier, J.N. (1970), *Theory of Elasticity*, McGraw-Hill, Tokyo, Japan.
Zhang, B.Y., Lv, M.Z. and Gao, L.S. (2003), "Correction of membrane penetration in large-scale triaxial tests for granular materials", *Wat. Res. Hydropow. Eng.*, **34**(2), 30-33.

CC